

## UNCERTAINTY QUANTIFICATION IN THE DYNAMICS OF WIND-TURBINE CURVED BLADES WITHIN THE FORMULATION OF ISO GEOMETRIC ANALYSIS

Diego E. Cardenas<sup>a</sup>, Marcelo T. Piovan<sup>b</sup>, Hugo R. Elizalde<sup>c</sup> and Oliver Probst<sup>d</sup>

<sup>a</sup> *Tecnológico de Monterrey, Escuela de Ingeniería y Ciencias, Avenida General Ramón Corona 2514, CP 45138, Zapopan, México.*

<sup>b</sup> *Centro de Investigaciones de Mecánica Teórica y Aplicada, Universidad Tecnológica Nacional FRBB. 11 de Abril 461, B8000LMI, Bahía Blanca. Argentina.*

<sup>c</sup>

*Tecnológico de Monterrey, Escuela de Ingeniería y Ciencias, Calle del Puente 222, CP 14380, Ciudad de México, México*

<sup>d</sup> *Tecnológico de Monterrey, Escuela de Ingeniería y Ciencias, Av. Eugenio Garza Sada 2051 Sur, CP 6484964849 Monterrey, Mexico*

**Keywords:** Iso-geometric analysis, composite curved beams, material uncertainties, stochastic modeling, dynamics, variable curvature.

**Abstract.** In this paper we study the dynamics of wind-turbine blades constructed with resin-fiber reinforced composites with uncertainties. The constructive process of these structures, although conceived to be carried out mostly with robust automatic machines, cannot avoid the presence of a number of details that lead to unexpected spurious mechanical behavior. In this type of structures the source of uncertainty can be found in geometric, material and mechanical aspects. In order to study the uncertain dynamics of these structures, we employed a composite curved beam model formulated in the context of iso-geometric analysis. The model incorporates, variable curvature and geometrical variability within the cross-section. It serves as a mean deterministic approach to the studies on stochastic dynamics and uncertainty quantification, which are objectives of this article. The computational procedure to quantify the uncertainty in the beam dynamics involves the introduction of random variables related to material or geometric properties such as elasticity moduli, material density, wall thickness and fiber angle along the axis of the beam. The probability density functions (PDF) of the random variables are derived appealing to the Maximum Entropy Principle according to given knowledge about the variability of the uncertain parameters. Then, a probabilistic model is constructed with the basis of the deterministic model and both discretized with finite element approaches. Once the probabilistic model is constructed, the plain Monte Carlo and a Latin Hypercube sampling are employed to carry out random realizations. With the aim to seek the sensitivity of the uncertain parameters, a number of possible scenarios are evaluated.

## 1 INTRODUCTION

The behavior of composite structures under service in aeronautical, aero-space or mechanical devices is subjected to a number of factors that are stochastic in essence. A number of researchers (Vickenroy and Wilde, 1995; Salim et al., 1993) started to evaluate the stochastic response of composite structures in the middle nineties. Moreover, there is a constant interest to quantify the propagation of uncertainty in the mechanics of composite materials at the microscale level (Sriramula and Chryssantopoulos, 2009) or for failure analysis (Pawar, 2011). The uncertainty connected with material properties of the composites can be considered as random fields according to the works Mehrez et al. (2012b) and Mehrez et al. (2012a) among others. However, there are many ways to take into account the uncertainty for studying the dynamic response of composite structures, for example by associating random variables to given entities that define a structural dynamic model. Actually, when parameters such as material properties or geometric features of the model, are considered uncertain, the stochastic methodology is called parametric probabilistic approach (PPA), Soize (2001). Using this approach Piovan and Sampaio (2015) among others have studied the propagation of uncertainty in the dynamics of composite beams, related to material parameters and some geometric parameters.

In this article, the PPA is applied in order to evaluate the uncertainty in the dynamic response of naturally curved non-uniform composite thin walled beams. The theory of the curved structure introduced by Cardenas et al (2018) in the conceptual frame of one dimensional Iso-Geometric Analysis (IGA) is employed here as a mean model. The solution of the dynamics equations is approximated by means of an IGA finite elements approach. For the PPA case, the parameters corresponding to elastic properties are considered uncertain. To construct the probabilistic models, the probability density functions associated with the random variables are constructed based on the Maximum Entropy Principle (Jaynes, 1957a,b). This principle uses the available information of the uncertain entities to construct their probability density functions such that their Entropy (defined according to Shannon, 1948) is the maximum. The use of this scheme allows the maximum possible propagation of the uncertainty according to the available information about the random variables.

The article is organized as follows: after the introductory section where the state-of-the-art in modeling curved thin walled composite beams with IGA is summarized, the deterministic/mean model and its finite element discretization are described. Afterward the probabilistic model is constructed assuming material properties, variable curvature and reinforcement angle as random variables. The subsequent section contains the computational studies, the analysis of the uncertainty propagation in the dynamics of thin walled composite curved beams. Finally some concluding remarks are outlined and future prospective offered.

## 2 GENERAL MODEL

### 2.1 Thin Walled BEM-IGA Model

The main governing assumptions of the composite thin-walled beam (TWB) here developed are: 1) small-strain linear field, 2) the beam conforms to an Euler-Bernoulli description, i.e., the beam's cross-section remains plane and undeformed in its own plane and perpendicular to the bending line after being displaced, 3) the Kirchhoff-Love assumption remains valid in classical laminated theory (CLT), and 4) the in-plane and warping shear strains are uniform over the cross-section and follow a linear variation through-the-thickness. In this section, the main equations governing the mechanics of rectilinear TWB are first presented according to the description in Zhang and Wang (2014) then transformed via the

Frenet-Serret frame field to yield correspondent equations for curved TWB.

### 2.1.1 Kinematics of rectilinear TWB

With reference to the nomenclature presented by Zhang & Wang (2014) and Figure 1, which depict both rectilinear and curved TWB, the displacement field of a TWB can be expressed with respect to the global coordinate system  $\mathbf{X}, \mathbf{Y}, \mathbf{Z}$  or with respect to the cross-section's coordinate system  $\mathbf{t}, \mathbf{n}, \mathbf{b}$ , which are equivalent for a rectilinear and curved axis. However, it is convenient to express the displacement field in terms of the shell's coordinate system  $\mathbf{s}, \mathbf{h}, \mathbf{t}$  whose axes are oriented along the counter-clockwise tangent ( $\mathbf{s}$ ), outward normal ( $\mathbf{h}$ ) and out-of-plane ( $\mathbf{t}$ ) directions with origin at an arbitrary location on the cross-section's mid-contour and with its  $\mathbf{t}$  axis parallel to the beam's  $\mathbf{t}$  axis. The fibre-direction  $\beta$  of a given layer is measured with respect to the  $\mathbf{s}$  axis, therefore  $0^\circ$  represent fibres aligned to the hoop ( $\mathbf{s}$ ) direction while  $90^\circ$  represent fibres aligned to the beam's axis ( $\mathbf{t}$ ).

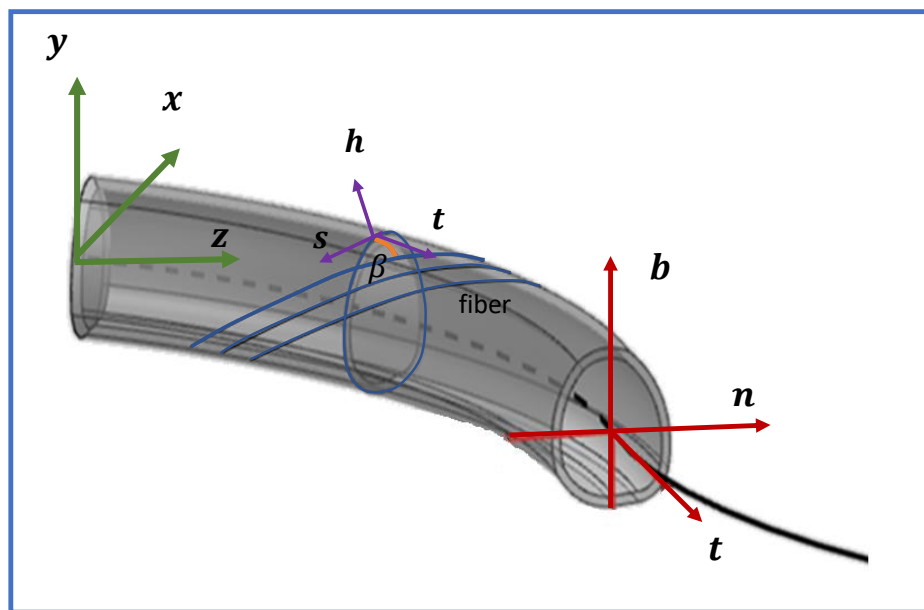


Figure 1. Coordinate systems for rectilinear and curved TWB

Figure 2 depicts a TWB's cross-section and its mid-contour following the nomenclature presented by Zhang & Wang (2014) equally valid for rectilinear and curved beams, also showing the auxiliary variables needed to transform between the  $(\mathbf{t}, \mathbf{n}, \mathbf{b})$  and  $(\mathbf{s}, \mathbf{h}, \mathbf{t})$  frames. To this end, coordinates  $n, b$  need to be expressed as functions of coordinates  $s, h$ , i.e.  $n(s, h), b(s, h)$ ; the barred variables  $\bar{n}(s) = n(s, 0)$  and  $\bar{b}(s) = b(s, 0)$  are analogous coordinates but measured along the mid-contour ( $h = 0$ );  $\alpha(s)$  is the angle measured from the positive direction of the  $\mathbf{n}$ -axis to the positive direction of the  $\mathbf{s}$ -axis, and  $r(s)$  and  $q(s)$  are auxiliary vectors aligned with the positive directions of axes  $\mathbf{s}$  and  $\mathbf{h}$ , respectively.

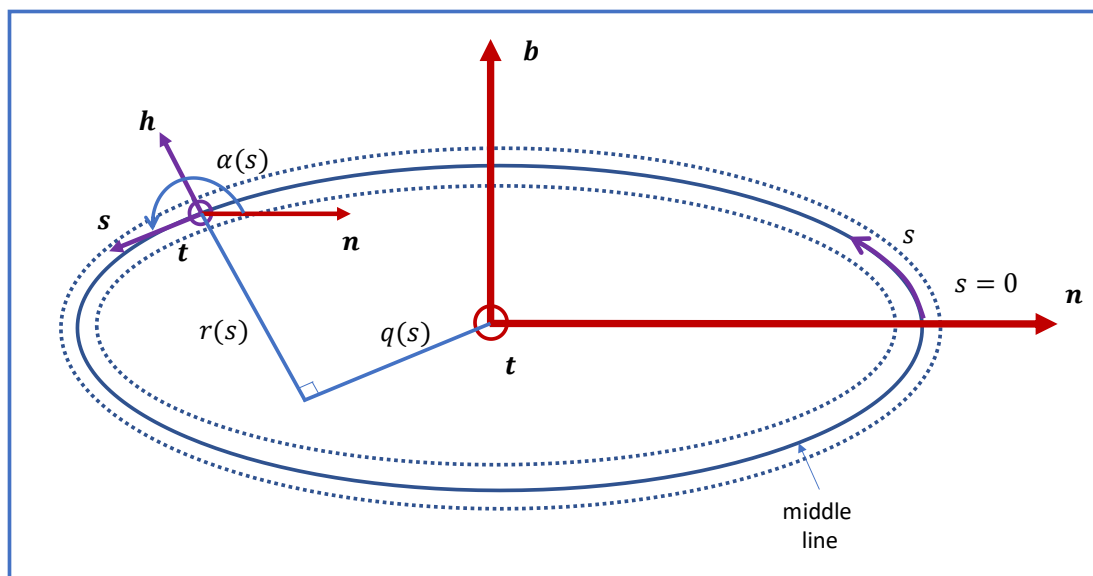


Figure 2. Cross-section's (i.e. Shell's) coordinate system  $\mathbf{s}, \mathbf{h}, \mathbf{t}$  and auxiliary variables. With the above definitions, the displacement  $\mathbf{u}(t)$  and rotational  $\boldsymbol{\theta}(t)$  fields of a TWB's rectilinear axis (i.e. the *pole line* used for referencing the beam's cross-section) can be expressed as:

$$\mathbf{u}(t) = u_t(t)\mathbf{t} + u_n(t)\mathbf{n} + u_b(t)\mathbf{b} \quad (1a)$$

$$\boldsymbol{\theta}(t) = \theta_t(t)\mathbf{t} + \theta_n(t)\mathbf{n} + \theta_b(t)\mathbf{b} \quad (1b)$$

where  $u_t(t)$  ( $\theta_t(t)$ ),  $u_n(t)$  ( $\theta_n(t)$ ) and  $u_b(t)$  ( $\theta_b(t)$ ) are scalar coordinates measured along the  $\mathbf{t}, \mathbf{n}, \mathbf{b}$  axes, respectively. The Euler-Bernoulli condition is satisfied if:

$$\theta_n(t) = -u_b'(t) \quad (2a)$$

$$\theta_b(t) = u_n(t) \quad (2b)$$

where the upper coma (') represents differentiation with respect to coordinate  $t$ . The displacement field of any point of the cross section of the TWB beam can be expressed in the  $\mathbf{s}, \mathbf{h}, \mathbf{t}$  frame as:

$$U_n = u_n - \theta_t(\bar{b} - h \cos \alpha) \quad (3a)$$

$$U_b = u_b + \theta_t(\bar{n} + h \sin \alpha) \quad (3b)$$

$$U_t = u_t - u_n'(\bar{n} + h \sin \alpha) - u_b'(\bar{b} - h \cos \alpha) - \omega \theta_t' \quad (3c)$$

where  $\bar{n}$  and  $\bar{b}$  are scalar coordinates measured along the  $s$  axis of the midline wall contour, and  $\omega(s)$  is a warping function defined in Zhang and Wang (2014). Following this reference, the strain field associated to Eq. (3) can be decomposed via the classical laminate theory (CLT) into mid-contour strains ( $\bar{\epsilon}_{tt}, \bar{\gamma}_{st}$ ) and associated curvatures ( $k_{tt}, k_{st}$ ):

$$\epsilon_{tt}(s, h, t) = \bar{\epsilon}_{tt}(s, t) + h k_{tt}(s, t) \quad (4a)$$

$$\gamma_{st}(s, h, t) = \bar{\gamma}_{st}(s, t) + h k_{st}(s, t) \quad (4b)$$

where:

$$\bar{\epsilon}_{tt}(s, t) = u_t'(t) + \bar{b}(s) \theta_n'(t) - \bar{n}(s) \theta_b'(t) - \omega(s) \theta_t''(t) \quad (5a)$$

$$k_{tt}(s, t) = -\cos \alpha(s) \theta_n'(t) - \sin \alpha(s) \theta_b'(t) + q(s) \theta_t''(t) \quad (5b)$$

$$\bar{\gamma}_{st}(s, t) = \psi(s) \theta_t'(t) \quad (5c)$$

$$k_{st}(s, t) = 2 \theta_t'(t) \quad (5d)$$

This concludes the review of the main kinematic equations of rectilinear TWB.

### 2.1.2 Kinematics of curved TWB

The displacement and strain field of Equations (3) to (5) was developed for a generic cross-section of a rectilinear TWB but it is equally valid for a curved TWB as long as all the derivatives with respect to  $t$ , represented by the upper-coma symbol ( $'$ ), are now calculated as total derivatives accounting for the rate of change caused by the curvature of coordinate  $t$ . This issue can be efficiently handled by using the Frenet-Serret frame field, which provides an orthonormal basis describing the geometric and kinematic properties of a non-degenerate but otherwise arbitrary curve in the Euclidean  $\mathfrak{R}^3$  space Zhang et al (2016). In Figure 3,  $\mathbf{t}$ ,  $\mathbf{n}$ ,  $\mathbf{b}$  are orthonormal unit vectors defining the tangent, normal and binormal directions at any point along the three-dimensional curve  $\mathbf{r}(t) = X(t)\mathbf{X} + Y(t)\mathbf{Y} + Z(t)\mathbf{Z}$  which, in the context of a curved TWB, represents the beam's pole;  $t$  is a scalar coordinate representing the curve's arc-length and scalars  $\kappa(t)$ ,  $\tau(t)$  are the in-plane curvature and out-of-plane torsion of the curve, respectively, both allowed to vary continuously as functions of coordinate  $t$ . Frenet-Serret frame provides an effective means for calculating the total derivative field of any vector quantity  $\mathbf{v}(t) = v_t(t)\mathbf{t} + v_n(t)\mathbf{n} + v_b(t)\mathbf{b}$  with respect to the arc-length  $t$ :

$$\begin{aligned} \frac{\partial \mathbf{v}(t)}{\partial t} = & \left( \frac{\partial v_t(t)}{\partial t} - \kappa(t)v_n(t) \right) \mathbf{t} + \left( \frac{\partial v_n(t)}{\partial t} + \kappa(t)v_t(t) - \tau(t)v_b(t) \right) \mathbf{n} \\ & + \left( \frac{\partial v_b(t)}{\partial t} + \tau(t)v_n(t) \right) \mathbf{b} \end{aligned} \quad (6)$$

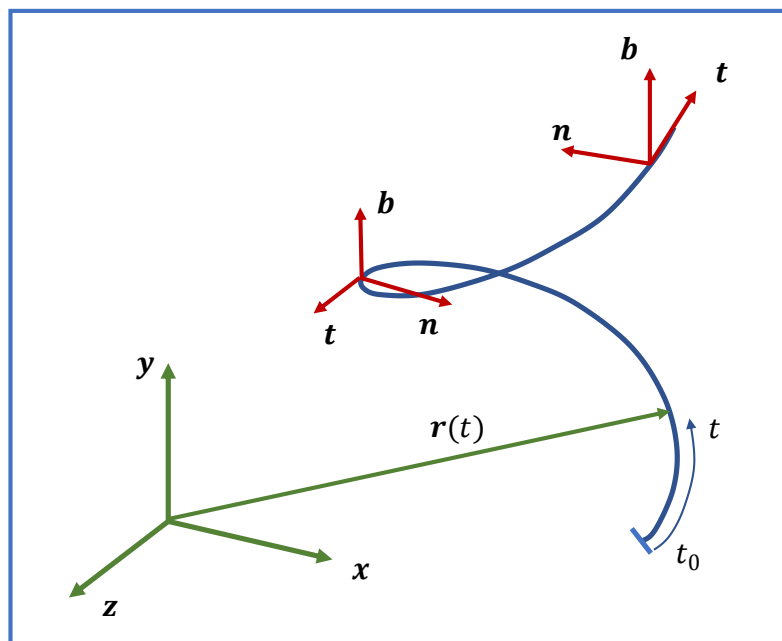


Figure 3. The Frenet-Serret frame field and associated nomenclature

Applying Eq. (6) to Eq. (3c) and (5), which also involves applying it to the Euler-Bernoulli condition of Eq. (2), the resulting displacement and deformation variables applicable to curved TWB. In the interest of brevity and because TWB structures with planar variable curvature (instead of a full 3D curvature) are far more common in structural applications, in the following the out-of-plane torsion  $\tau$  and its derivatives will be equated to zero to allow the analysis of more compact equations. Further details on the displacement and deformation field expressed in a Frenet-Serret frame and the implementation of an isogeometric scheme to obtain the stiffness and mass matrices of a TWB, review the work of Cardenas et al. (2018).

## 2.2 Construction of the Parametric Probabilistic Model

In the previous section the deterministic model of a composite thin-walled curved beam formulated in the IGA background has been introduced. The probabilistic model is here constructed from the finite element equation of the deterministic model/mean. Now, taking into account that a number of parameters may have different levels of variability, leading to an uncertain behavior in the curved beam motion, in this section some guidelines are established to quantify the uncertainty aspects of the mathematical model. The PPA implies the selection of a set of parameters of the structural member that are assumed to be uncertain and random variables are associated with them. According to the authors' opinion, the Maximum Entropy Principle (MEP) facilitates the construction of a probabilistic model by offering the background to derive the probability distribution function (PDF) of given random variables despite the lack of knowledge about uncertainty levels (Shanon, 1948). Thus PDF can be deduced guaranteeing consistence with the physics of the problem and the available information.

In order to deduce the PDF of the random variables the following conditions are proposed:

- Random variables related to material properties are positive and have bounded supports
- Random variables associated with reinforcement angles or geometric parameters have bounded supports whose upper and lower limits are distant from the expected value a given quantity
- The expected values of the random parameters are the nominal values of the deterministic model.
- The variance of the random variables must be kept finite for the physical consistency the problem
- No information is given about the correlation among random variables.

Thus employing the MEP (Shanon, 1948; Soize, 2001; Piovan and Sampaio, 2015) constrained to the previous conditions, on arrives to the following PDF form the random variables associated with material properties and some geometric entities.

$$p_{V_i}(v_i) = 1_{[L_{V_i}, U_{V_i}]}(v_i) \frac{1}{U_{V_i} - L_{V_i}}, i = 1, 2, \dots \quad (7)$$

Which is a uniform distribution.  $1_{[L_{V_i}, U_{V_i}]}$  is a generic support function and  $L_{V_i}$  and  $U_{V_i}$  are the lower and upper bounds of the uniform distribution related to the  $i$ -th random variable. Matlab function `unifrnd(LVi, UVi)` is used in this work. These bounds can be defined in terms of central and dispersion measures like expected value  $\bar{V}_i$  and coefficient of variation  $\delta_i$  as:

$$\begin{aligned} L_{V_i} &= \bar{V}_i(1 - \delta_i\sqrt{3}) \\ U_{V_i} &= \bar{V}_i(1 + \delta_i\sqrt{3}) \end{aligned} \quad (8)$$

## 3 CASE STUDY

The case study was selected to test the dynamic capabilities of the TWB model under uncertainty scenarios. To this end, a wind turbine blade with planar variable axial curvature, complex geometry, aerodynamic cross-section and orthotropic material layup along the perimeter was modelled as shown in Figures 4. The radius of the planar curved axis follows a

parabolic path (Fig. 4a) described by the equation  $radius = -0.296H^2 + 0.889H + 0.333$ , spanning a maximum height of  $H = 3$  m and a total arc-length of  $t_{max} = 3.36$  m. The cross-section corresponds to a NACA 0015 profile with a chord of 75 mm (Fig. 4b). The blade's boundary conditions include fixtures at both ends and unitary punctual force applied at an arc-length of  $\xi = 0.5$  (that is, at the blade's mid-length) for each of the three-coordinate system direction (X-Y-Z)

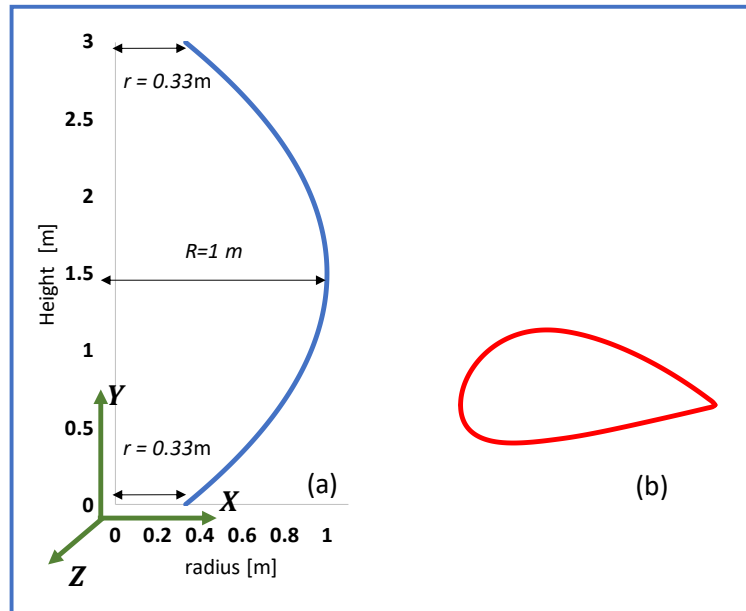


Figure 4. Blade geometry. a) pole line and b) Cross section profile (NACA 0015)

### 3.1 Uncertainty Scenarios

The manufacturing process of wind turbine blades presents various sources of uncertainty with respect to design values. The manual labor still present on the process is the main reason. In this numerical experiment, it is analyzed the effect of uncertainty on the dynamic response of the structure due to the following variables: fiber angle, Young's Modulus and laminate thickness. Six different cases are run varying the fiber orientation:  $[0^\circ, 30^\circ, 45^\circ, 60^\circ, 75^\circ, 90^\circ]$  all of them with a single layer of 4 mm and the material described on Table 1.

Material Properties	Glass Fiber (C520)
$E_{11}$ [MPa]	1900
$E_{22}$ [MPa]	26.9
$E_{12}$ [MPa]	131
$\nu_{12}$	599

For each fiber orientation, 1000 simulations were performed varying the angle orientation  $\pm 10^\circ$ , laminate thickness 20% and Young Modulus 30%, following Eq. 11 and 12. For each simulation the firsts 4 natural frequencies and FRF are calculated.

### 3.2 Results

Fig. 5 shows the scaled distribution of the natural frequencies of the first 4 modes for the 1000 simulations performed for each fiber orientation value ( the distribution color represents the fiber orientation). In the secondary axis of the Fig. 5, the standard deviation of the natural

frequency is plotted due to the uncertainty present in the considered variables. It can be observed for the same mode, as the fiber is oriented from the perimeter ( $0^\circ$ ) to the axis of the beam ( $90^\circ$ ) the natural frequency increases, due to the stiffening of the beam. As the fiber is oriented toward the axis of the beam, the uncertainty causes greater variation in the natural frequency. Also, for higher modes the dispersion increases.

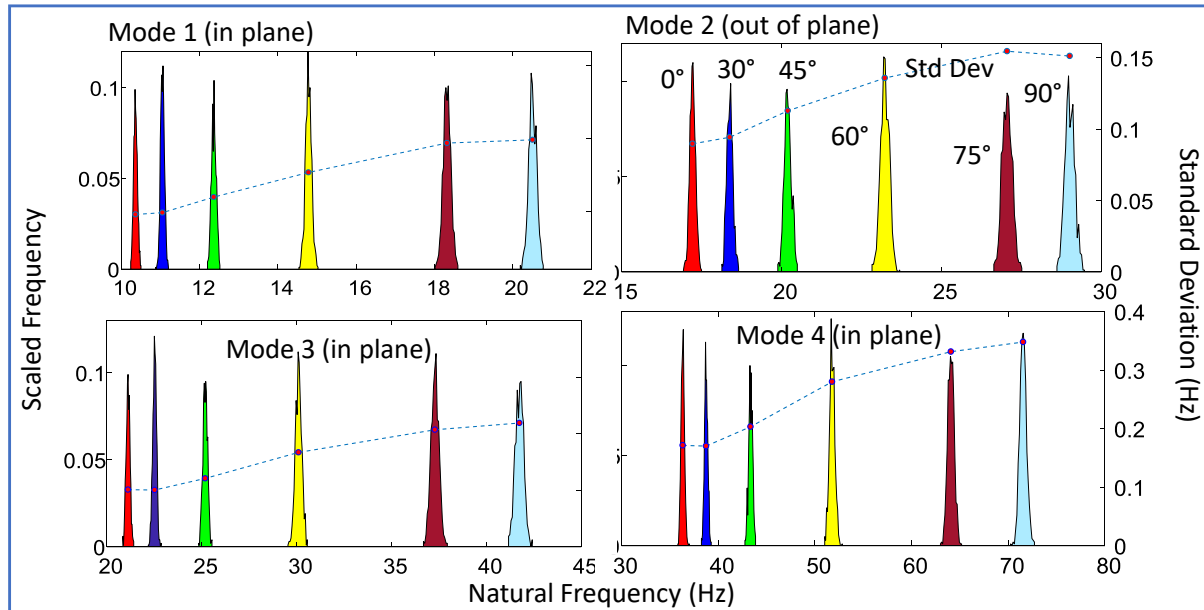


Figure 5. Natural Frequencies histograms

In Fig. 6 can be observed the frequency response in X direction measured at the center of the blade for a unit load applied in the same position and direction. Each color corresponds to a different fiber orientation, the solid line represents the deterministic response of the model, and the dashed line and dotted line are the maximum and minimum values present in the 1000 simulations performed for each fiber orientation case. Fig. 7 and 8 correspond to FRF to Y and Z directions respectively. In the three FRFs we can see the same effect described in Fig. 5. As the fiber aligns from the perimeter of the section to the axis of the beam the effect of the uncertainty increases. It can be noticed for the case of  $90^\circ$ , the distance between the maximum and minimum curves is the wider, besides the both curves are shifted to the left compared to the deterministic response.

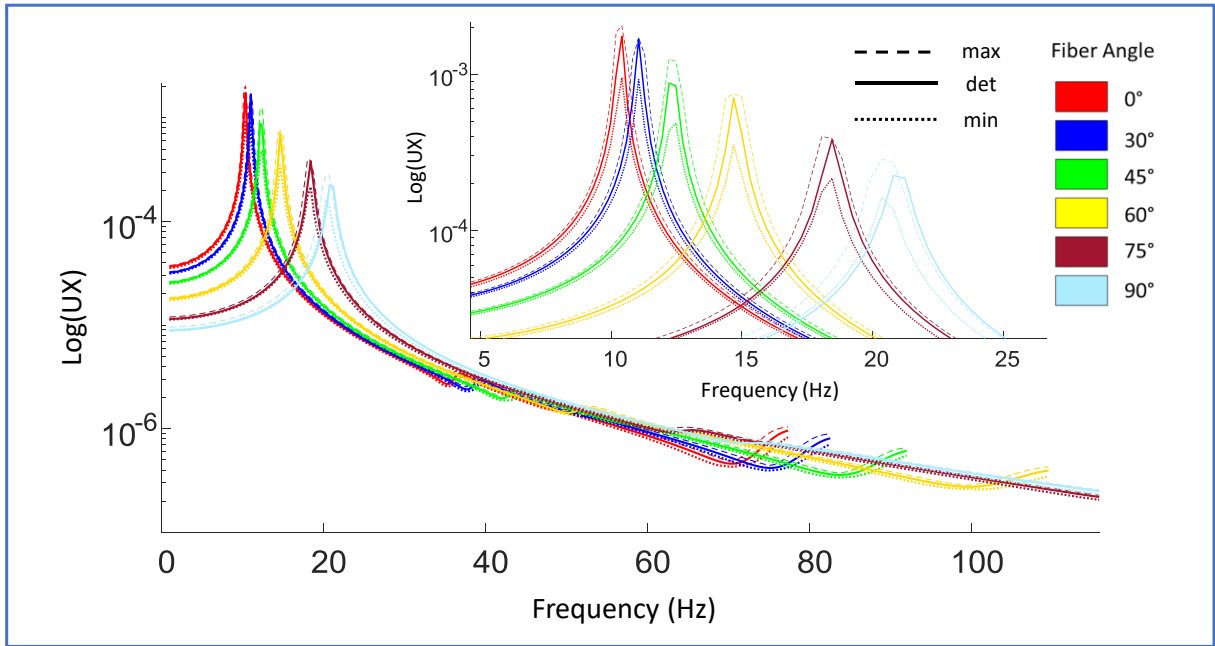


Figure 6. FRF force applied in X direction

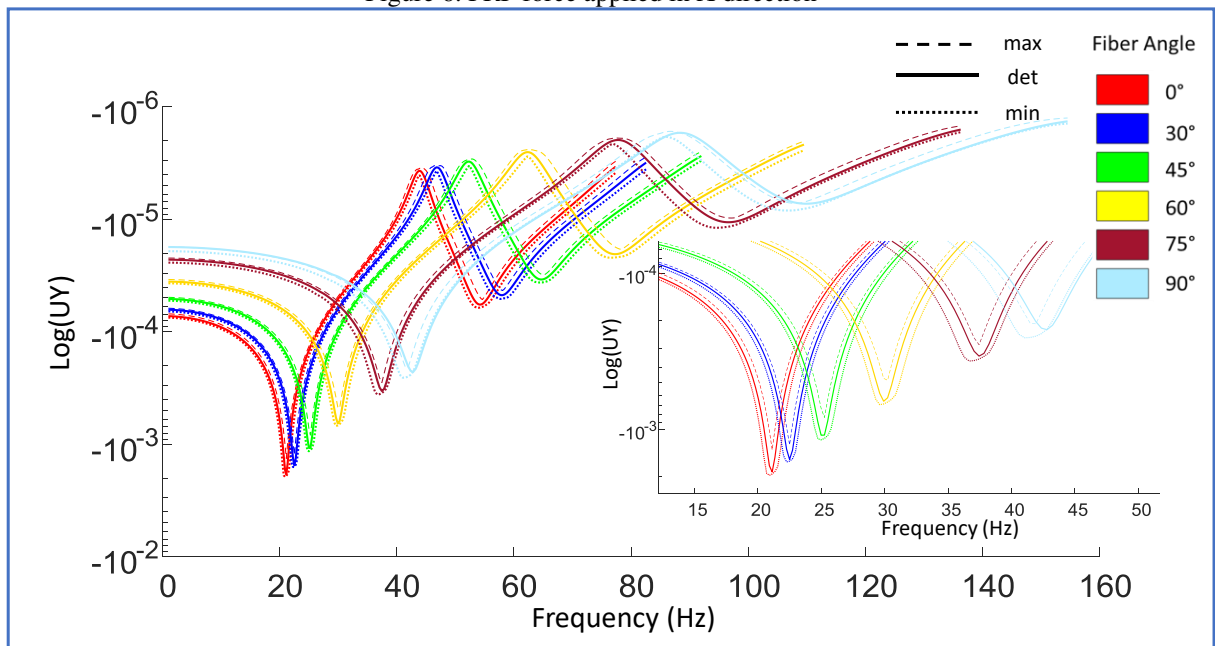


Figure 7. FRF force applied in Y direction

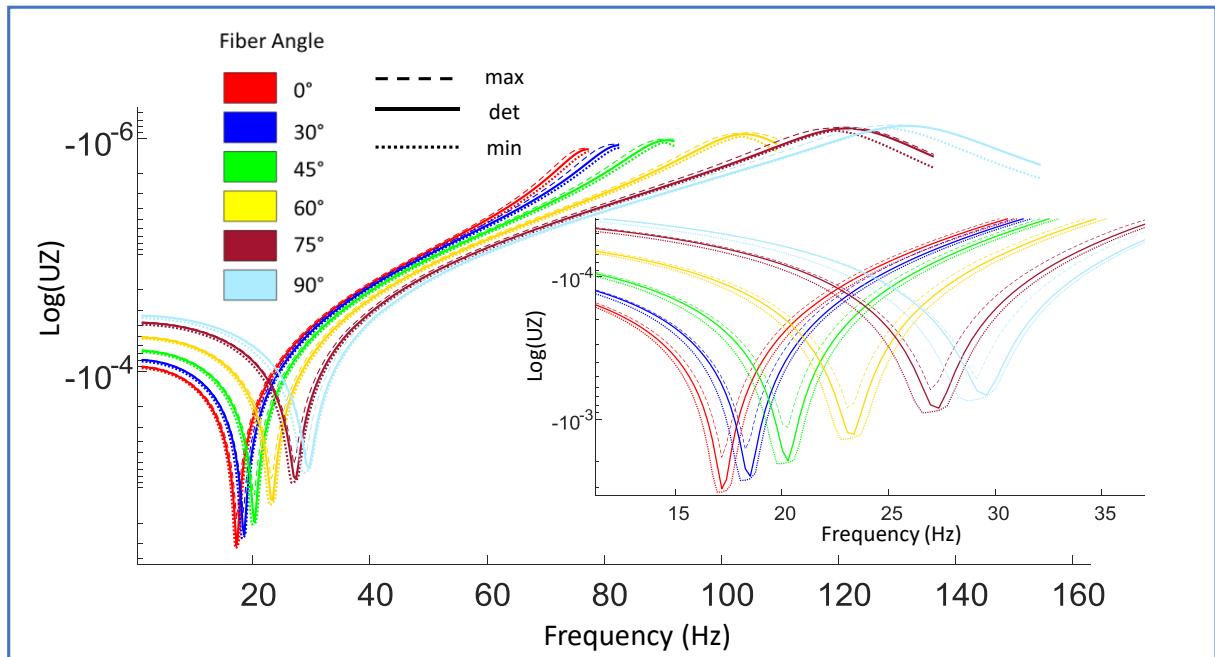


Figure 8. FRF force applied in Z direction

## CONCLUSIONS

In this paper the dynamics of wind-turbine blades constructed with resin-fiber reinforced composites with uncertainties were studied. Due the manufacturing process to fabricate wind turbine blades includes some manual tasks, variations in the mechanical properties of the material, thickness of the laminates and the orientation of the fiber were considered. In order to study the uncertain dynamics of these structures, it was employed a composite curved beam model formulated in the context of iso-geometric analysis. The model incorporates, variable curvature and geometrical variability within the cross-section. The probability density functions (PDF) of the random variables are derived appealing to the Maximum Entropy Principle according to given knowledge about the variability of the uncertain parameters. Then, a probabilistic model is constructed with the basis of the deterministic model and both discretized with finite element approaches. It was observed that the uncertainty on the considered parameters have different depending on the orientation of the fiber laminate. The effects are greater when the fiber is aligned to the axis of the beam.

## REFERENCES

- Cardenas D., Elizalde H., Jauregui J., Piovan M.T., Probst O. Unified Theory for Curved Composite Thin-Walled Beams and its Isogeometrical Analysis. *Thin-Walled Structures*, on press, 2018.
- Pawar P. On the behavior of thin walled composite beams with stochastic properties under matrix cracking damage. *Thin-Walled Structures*, 49:1123–1131, 2011.
- Piovan M.T. and Sampaio R. Parametric and non-parametric probabilistic approaches in the mechanics of thin-walled composite curved beams. *Thin-Walled Structures*, 90:95-106, 2015.
- Salim S., Yadav D., and Iyengar N. Analysis of composite plates with random material

- characteristics. *Mechanics Research Communications*, 20(3):405–414, 1993.
- Sampson W. *Modelling stochastic fibrous materials with Mathematica*. Springer-Verlag London Limited, 2009.
- Shannon C. A mathematical theory of communication. *Bell Systems Tech*, 27:379–423, 1948.
- Soize C. Maximum entropy approach for modeling random uncertainties in transient elastodynamics. *Journal of the Acoustical Society of America*, 109(5):1979–1996, 2001.
- Sriramula, S., Chryssantopoulos, M. Quantification of uncertainty modelling in stochastic analysis of composites. *Composites: Part A* 40:1673–84, 2009.
- Vickenroy G. and Wilde W. The use of the Monte Carlo techniques in statistical finite element methods for the determination of the structural behavior of composite material structural components. *Composite Structures*, 32(1), 1995.
- S. Wang, C. Zhang, Structure mechanical modeling of thin-walled closed-section composite beams, Part 1: Single-cell cross section, *Compos. Struct.* 113 (2014) 12–22. doi:10.1016/j.compstruct.2014.03.005.
- S. Wang, C. Zhang, Structure mechanical modeling of thin-walled closed-section composite beams, part 2: Multi-cell cross section, *Compos. Struct.* 113 (2014) 56–62. doi:10.1016/j.compstruct.2014.03.002.
- G. Zhang, R. Alberdi, K. Khandelwal, Analysis of three-dimensional curved beams using isogeometric approach, *Eng. Struct.* 117 (2016) 560–574. doi:10.1016/j.engstruct.2016.03.035.